

Reproduction of inequality constraint between iron and silica for accurate production scheduling

S Abulkhair¹, N Madani² and N Morales³

1. Research Assistant, School of Mining and Geosciences, Nazarbayev University, 010000 Nur-Sultan, Kazakhstan. Email: sultan.abulkhair@nu.edu.kz
2. Assistant Professor, School of Mining and Geosciences, Nazarbayev University, 010000 Nur-Sultan, Kazakhstan. Email: nasser.madani@nu.edu.kz
3. Director, Delphos Mine Planning Lab, AMTC and Department of Mining Engineering, University of Chile, 8370451 Santiago, Chile. Email: nelson.morales@amtc.cl

ABSTRACT

Conventional geostatistical algorithms cannot reproduce bivariate complexities such as inequality constraint, nonlinearity and heteroscedasticity. Poor reproduction of these features may decrease the accuracy and reliability of mine planning results. For example, it is not unusual to have an inequality constraint between primary and disturbing elements in a metalliferous deposit. Implementation of traditional methodologies for such complex data sets can lead to the incorrect reproduction of a bivariate relationship, which will affect the validity of NPV results. In this paper, an iron data set containing iron and silica grades with an inequality constraint between variables is introduced as a case study. This study proposes an algorithm based on a hierarchical sequential Gaussian cosimulation integrated with inverse transform sampling. The proposed methodology considers the linear inequation between two variables in the hierarchical cosimulation process to reproduce an inequality constraint. As a comparison, conventional sequential Gaussian cosimulation is also applied to the same data set to demonstrate the difference in bivariate relationships from both models. Unlike the proposed algorithm, the conventional cosimulation cannot reproduce an inequality constraint and slightly overestimates silica grades. The modelled realisations are then used to assess the uncertainty of a plan and generate a stochastic strategy that adapts the destination of the blocks depending on the scenario. Two-stage stochastic long-term production scheduling takes extraction decisions using average information (ie e-type model) and ore/waste destinations based on geostatistical realisations. As a result, the proposed strategy is closer to the upper bound, highest possible NPV for each realisation, than to the lower bound, deterministic strategy that does not manage the risk of sending extracted material to wrong destinations. Furthermore, Comparing production schedules resulting from proposed and conventional geostatistical methodologies shows the importance of inequality constraint reproduction and more accurate long-term mine planning.

INTRODUCTION

The objective of long-term production scheduling in open pit mines is to generate a life-of-mine schedule with defined extraction periods and destinations for each mining block, while maximising net present value (NPV) and respecting operational constraints. Mixed integer programming (MIP) (Gershon, 1983) is a popular production scheduling approach used in the industry. Nevertheless, despite its effectiveness in maximising NPV and producing optimal solutions, it uses a single block model as an input. As a result, such deterministic mine planning methodologies can not control the deviations from production targets, leading to a high risk of not meeting them. Alternatively, using geostatistical realisations produced by simulation/cosimulation methodologies as inputs in MIP leads to suboptimal results (Ramazan and Dimitrakopoulos, 2004). Therefore, stochastic production scheduling approaches are required to effectively minimise the risk of not meeting production targets, maximise NPV and satisfy operational constraints.

Stochastic production scheduling approaches, such as simulated annealing (Godoy and Dimitrakopoulos, 2004) and stochastic integer programming (SIP) (Ramazan and Dimitrakopoulos, 2018), aim to produce optimal solutions with maximised NPV and minimised risks by using multiple unbiased scenarios of the economic block model. Simulated annealing can help to generate a 26 per cent higher NPV than the deterministic method (Leite and Dimitrakopoulos, 2007), but SIP can also make optimal waste removal decisions (Dimitrakopoulos, 2011). However, the integration

of uncertainty into stochastic mine planning approaches sometimes leads to a higher number of binary variables. One solution for this issue is replacing some variables with continuous ones and assigning binary variables only to waste blocks (Ramazan and Dimitrakopoulos, 2013). On the other hand, a two-stage stochastic production scheduling (Moreno *et al*, 2017) can be used as a more scalable alternative. In that approach, the first stage produces scheduling based on average information, similar to the deterministic method. The second stage corresponds to resource decisions taken using geostatistical realisations as different equally possible scenarios. According to Moreno *et al* (2017), extraction decisions should be taken in the first stage, while processing decisions – in the second.

Another problem with long-term production scheduling is the limited amount of information that mostly comes from exploration boreholes. Geostatistical resource modelling aims to generate spatially accurate models of mineral grades and geological domains using borehole data (Journel, 1999). In deposits containing multiple sampled elements, the spatial correlation between variables is a crucial source of information. Multivariate geostatistics considers the cross-covariances between variables to produce more valid models (Wackernagel, 2003). Nevertheless, traditional multivariate methods struggle to reproduce bivariate complexities, such as nonlinearity, heteroscedasticity and inequality constraints. It is particularly true for inequality constraints, which are common in mining deposits. Several methods based on the decorrelation of variables have been developed for the specific cases involving inequality constraints (Emery, Arroyo and Peláez, 2014; Arcari Bassani, Costa and Deutsch, 2018; Abildin, Madani and Topal, 2019). Recently, Madani and Abulkhair (2020) proposed a new methodology based on the acceptance-rejection technique integrated into hierarchical cosimulation. However, an acceptance-rejection technique iteratively re-simulates values that are outside an inequality constraint, making this algorithm much slower than traditional cosimulation. Therefore, Abulkhair and Madani (2021) replaced this method with an inverse transform sampling that makes only one iteration to re-simulate faulty values (ie values that are outside an inequality constraint).

This study demonstrates the performance of two-stage production scheduling and updated hierarchical cosimulation integrated with inverse transform sampling. Inverse transform sampling helps to re-simulate values, which do not respect an inequality constraint. Moreover, the proposed production scheduling approach evaluates fixed production periods using an average (ie e-type) resource model in the first stage, and then re-evaluates block destinations based on geostatistical realisations as the second stage decisions.

METHODOLOGY

Hierarchical cosimulation integrated with inverse transform sampling

The proposed cosimulation algorithm is an updated version of hierarchical sequential Gaussian cosimulation (Almeida and Journel, 1994). The basic idea of this algorithm is to simulate coregionalised variables hierarchically: the variable with the most autocorrelation is simulated first and then secondary variables are simulated conditional to the previous simulation results. This study is inspired by hierarchical cosimulation developed by Madani and Abulkhair (2020), in which an acceptance-rejection method integrated into the second simulation helps to model the secondary variable within an inequality constraint. However, an inverse transform sampling approach is used in this study as a faster alternative, while multiple and multicollocated neighbourhood strategies are implemented in the first and second simulations, respectively. For brevity, the readers are referred to both of these papers (Almeida and Journel, 1994; Madani and Abulkhair, 2020) to understand the basic methodology of hierarchical cosimulation, while the whole algorithm is proposed in Abulkhair and Madani (2021). The following steps demonstrate the procedure of an inverse transform sampling in detail:

1. Back transform simulated normal scores of the primary variable $Z_1^n(x_i)$ (ie variable modelled during the first simulation) to the original scale $Y_1^n(x_i)$ for each block i in n realisations.
2. Obtain the maximum max and minimum min truncated thresholds of the secondary variable $Y_2^n(x_i)$ based on the primary variable $Y_1^n(x_i)$. In the case of negative inequation, where $Y_2^n(x_i) \leq a \cdot Y_1^n(x_i) + b$, $[min, max]$ intervals are identified as follows:

$$\min^n(x_i) = \min(Y_2) \quad \max^n(x_i) = a \cdot Y_1^n(x_i) + b \quad (1)$$

Where:

- $\min(Y_2)$ is a minimum value of the secondary variable
- a is a slope
- b is an intercept.

3. Transform $\min^n(x_i)$ and $\max^n(x_i)$ thresholds into normal scores.
4. Identify values of the secondary variable that are not located within $[\min, \max]$ interval and store them as $Z_2^m(x_i)$.
5. Generated random numbers within truncated thresholds $V^m(x_i)$ using an inverse transform sampling (Devroye, 1986):

$$V^m(x_i) = F^{-1}(F(\min^m) + (F(\max^m) - F(\min^m)) \cdot U) \quad (2)$$

Where:

- F^{-1} is a quantile function
- F is a conditioned cumulative distribution function
- U is a random number generated uniformly between 0 and 1.

6. Re-simulate values $Z_2^m(x_i)$ identified in step 3 using random numbers $V^m(x_i)$ in the following way:

$$Z_2^m(x_i) = Z_{2MCKK}(x_i) + \sqrt{\sigma_{2MCKK}^2(x_i)} \cdot V^m(x_i) \quad (3)$$

Where:

- $Z_{2MCKK}(x_i)$ is a simple multicollocated co-kriging estimator
- $\sigma_{2MCKK}^2(x_i)$ is the corresponding estimation variance.

7. Loop to re-simulate all values identified in step 3.
8. Store re-simulated values in $Z_2^n(x_i)$.
9. Back transform simulated values of the primary and secondary variables into the original scale Y_1^n and Y_2^n .

Two-stage stochastic long-term production scheduling

This study implements two-stage stochastic production scheduling that employs average information from e-type models into the first stage, while the second stage decisions are based on geostatistical realisations. Production periods are computed in the first stage and are fixed for all realisations. Alternatively, second stage decisions focus on the re-evaluation of block destinations depending on mineral grades simulated by stochastic geostatistical methods. Integration of uncertainty into the second stage minimises the risk of sending the extracted material to the wrong destinations. The workflow of the proposed production scheduling methodology is the following:

1. Obtain economic block values $EBV(x_i)$ for e-type models and geostatistical realisations accounting on the impurity content of ore as follows:

$$EBV_\alpha = \max((P - C_S) \cdot R \cdot TON_\alpha * Y_{1\alpha} - (C_M + C_P) \cdot TON_\alpha - (Y_{2\alpha} > Y_2^{TH}) \cdot C_I \cdot (Y_{2\alpha} - Y_2^{TH}) \cdot TON_\alpha, -C_M \cdot TON_\alpha) \quad (4)$$

Where:

- P is a metal price
- C_S is a selling cost
- R is a recovery rate

C_M	is a mining cost
C_P	is a processing cost
TON_α	is a total tonnage for block α
C_I	is cost associated with an impurity content
Y_2^{TH}	is a threshold of the secondary variable, below which no impurity-related cost is applied.

2. Compute ultimate pit limit (UPL) and nested pits from e-type models using a pseudoflow algorithm (Hochbaum, 2008).
3. Define grade blending, mining, processing, reserve and operational constraints for the MIP.
4. Define pushbacks by grouping nested pits from a deterministic model and then selecting groups with similar tonnages.
5. First stage decisions: Compute production periods from e-type models using MIP with the following formulations:

$$\max \sum_{p \in P} \frac{EBV_{\alpha\tau}}{(1+d)^\tau} \cdot X_{\alpha\tau} \quad (5)$$

$$\sum_{\alpha \in A} X_{\alpha\tau} = 1 \quad \forall \alpha \in A, \tau \in T \quad (6)$$

$$\sum_{\alpha \in A} (Y_{1\alpha} - Y_1^{TH}) \cdot OTON_\alpha \cdot X_{\alpha\tau} \geq 0 \quad \forall \alpha \in A, \tau \in T \quad (7)$$

$$\sum_{\alpha \in A} TON_\alpha \cdot X_{\alpha\tau} \leq CAP_M^{max} \quad \forall \alpha \in A, \tau \in T \quad (8)$$

$$\sum_{\alpha \in A} OTON_\alpha \cdot X_{\alpha\tau} \leq CAP_P^{max} \quad \forall \alpha \in A, \tau \in T \quad (9)$$

Where:

d	is a discount rate
$\alpha \in A$	is a set of blocks
$\tau \in T$	is set of production periods
$X_{\alpha\tau}$	is an integer variable that is equal to 1 if a block α is extracted in a period τ and 0 if not
$Y_{1\alpha}$	is the primary variable
Y_1^{TH}	is a minimum threshold of the primary variable
$OTON_\alpha$	is an ore tonnage
CAP_M^{max} and CAP_P^{max}	are maximum thresholds of mining and capacities

Equation 6 is a reserve constraint

Equation 7 is a grade blending constraint

Equations 8–9 are mining and processing capacity constraints.

6. Re-evaluate tonnages TON_α^n and economic block values EBV_α^n based on n geostatistical realisations.
7. Second stage decisions: Re-evaluate the block destinations BD_α^n using grades from geostatistical realisations.

CASE STUDY

Proposed geostatistical and production scheduling methodologies are tested on a real data set from an iron deposit, which was multiplied by a scale factor to preserve confidentiality. The data set is homotopic and consists of 2137 sample points with coregionalised iron and silica variables. Figure 1a shows the location map of the data set used in this study. A critical feature of this deposit is a sharp inequality constraint between iron and silica (Figure 1b). Inequality constraint has a slope

a of -1.465 and an intercept b of 70.316, meaning that linear inequation for the proposed cosimulation algorithm is as follows:

$$\text{Silica} \leq 70.316 - 1.465 \cdot \text{Iron} \quad (10)$$

Furthermore, considering that the sampling pattern is slightly irregular (ie samples are mostly taken from the central part), cell-declustering is performed with 50 m × 50 m × 10 m cell dimension (Deutsch, 1989). Table 1 provides declustered statistical parameters of this deposit. Aside from an apparent inequality constraint, the correlation coefficient between variables is high. Therefore, conventional cosimulation is not likely to produce a significant overestimation of silica.

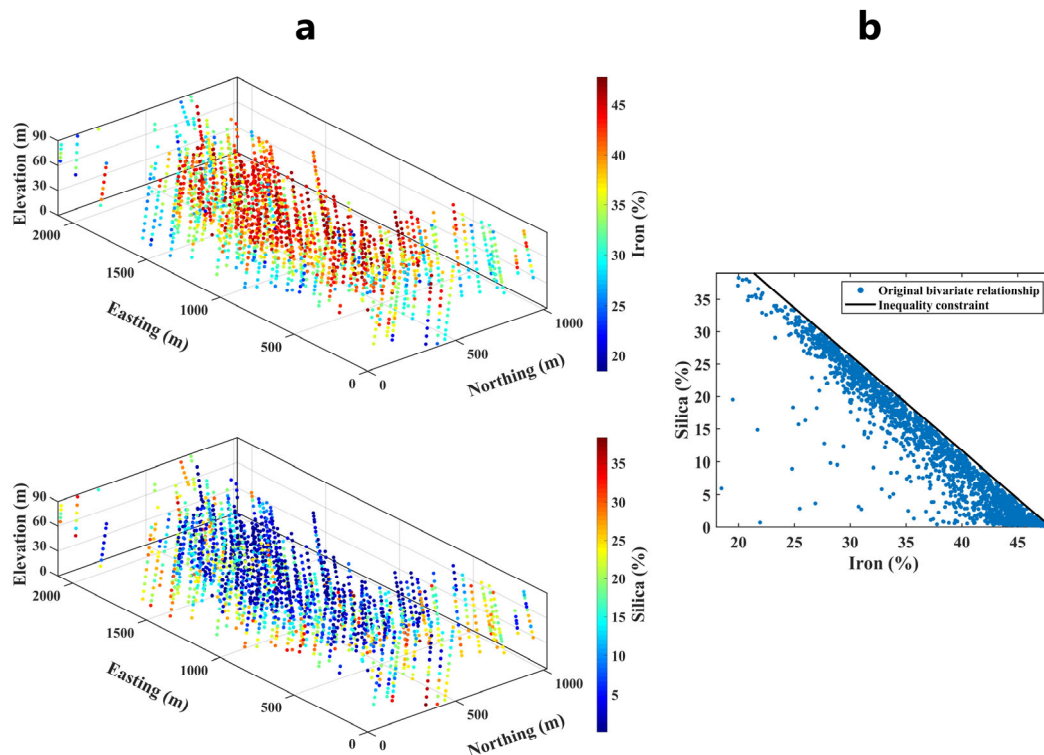


FIG 1 – (a) Location maps of iron and silica; and (b) a scatter plot between variables with a black line representing an inequality constraint.

TABLE 1

Basic declustered statistical parameters.

Statistical parameter	Iron (%)	Silica (%)
Mean	37.54	11.96
Variance	42.90	96.04
Correlation coefficient	-0.95	

Cosimulation of grade variables

In order to provide unbiased results for this case study, 100 realisations are produced using the proposed hierarchical cosimulation. The grid dimension of a single mining block is 20 m × 20 m × 10, which is used for both geostatistical modelling and production scheduling. Before proceeding to the cosimulation process, variables are transformed into normal scores. Then, direct and cross-variograms are calculated in the horizontal and vertical directions after examining an anisotropy. Finally, the following two-structured linear model of coregionalisation is obtained using a manual fitting:

$$\begin{pmatrix} \gamma_{Iron} & \gamma_{Iron/Silica} \\ \gamma_{Silica/Iron} & \gamma_{Silica} \end{pmatrix} = \begin{pmatrix} 0.25 & -0.17 \\ -0.17 & 0.18 \end{pmatrix} Exp(35m, 35m, 35m) + \begin{pmatrix} 0.65 & -0.66 \\ -0.66 & 0.73 \end{pmatrix} Exp(180m, 180m, 120m) \quad (11)$$

Figure 2 demonstrates e-type models, in which all blocks contain average grades of iron and silica over 100 realisations. Overall, results are compatible with location maps of original borehole data (see Figure 1a). The central part of the deposit contains high-grade iron and low-grade silica, meaning that a negative correlation between variables is reproduced. In fact, the simulated correlation coefficient between iron and silica is -0.93. Moreover, the average grades over 100 realisations are 36.50 per cent for iron and 11.06 per cent for silica, meaning that results are close to the original declustered parameters.

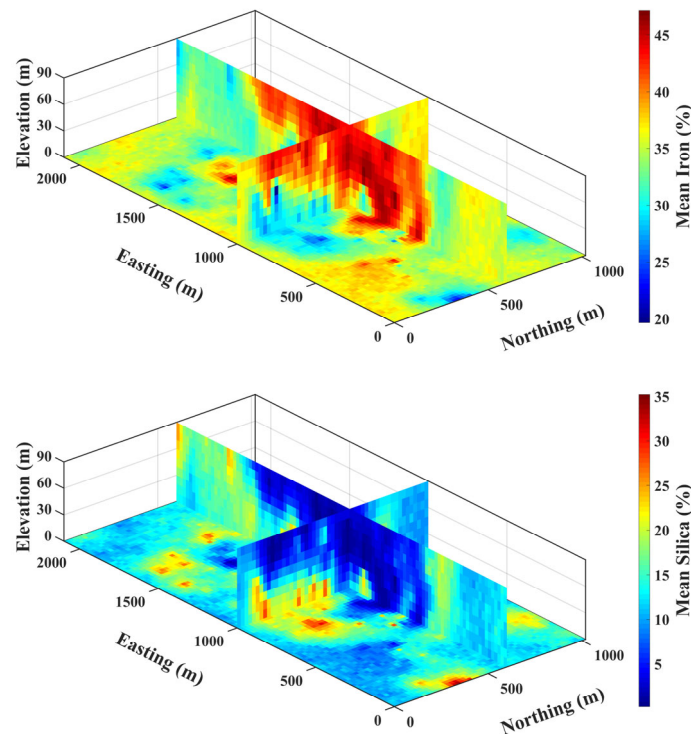


FIG 2 – E-type models over 100 realisations of iron (top) and silica (bottom).

It is of interest to compare the results with models obtained by the conventional methodology. The only difference between the two algorithms is the integration of an inverse transform sampling into the proposed method. Since an inverse transform sampling is implemented on the values computed during the second simulation, iron realisations are identical in both methods. However, the conventional method slightly overestimates silica that has an average grade of 13.40 per cent. Furthermore, the average correlation coefficient in realisations produced by the conventional method is -0.91. Although differences are not critical, it is better to analyse the bivariate relationships. Figure 3 shows how scatter plots between iron and silica are reproduced by two methodologies in realisation No. 1. Simulated bivariate relationships between variables and their marginal distributions are compared to the original parameters in Figure 3a. It should also be mentioned that scatter plots from block models are subsampled to show only 3000 random block values for a more valid comparison. Inverse transform sampling helps to reproduce an inequality constraint perfectly (see Figure 3c), while conventional methodology predictably fails to model this feature (see Figure 3b). Traditional Gaussian-based cosimulation methodologies model the bivariate relationships between coregionalised variables using only their cross-correlation structure. Inverse transform sampling in the proposed algorithm acts as an additional restriction that re-simulates all faulty values to reproduce an inequality constraint. Therefore, the conventional method can show much worse results in deposits with a lower cross-correlation and more skewed marginal distributions (Abulkhair and Madani, 2021).

Another important detail is that the histogram validation of silica realisations demonstrates that the re-simulation of silica values does not negatively affect its marginal distribution. This is because the proposed algorithm only re-simulates values that lie outside the threshold defined by inequation. On the contrary, silica's histogram from the proposed method has a closer resemblance to the original marginal distribution thanks to the re-simulation of overestimated values.

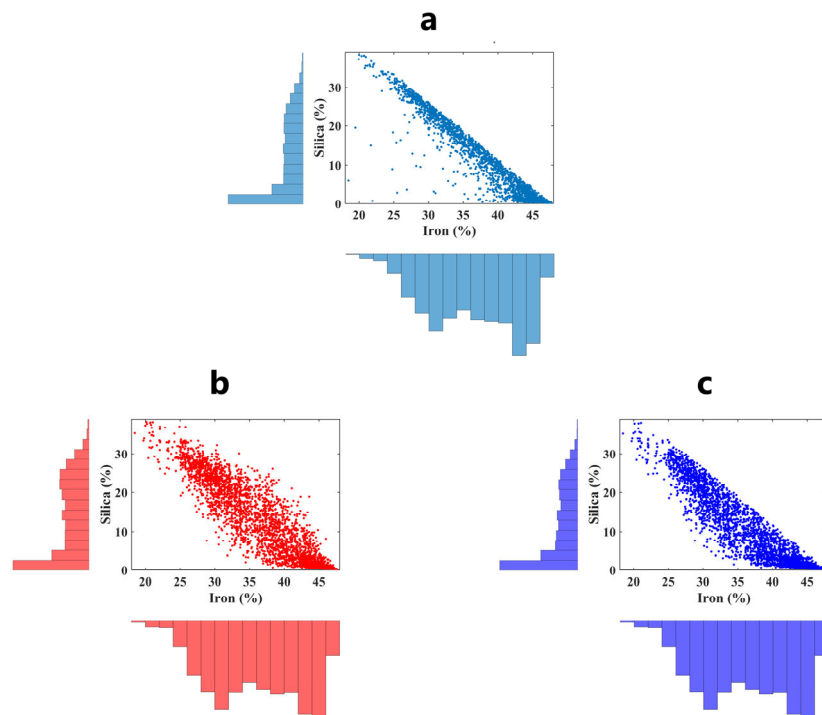


FIG 3 – The bivariate relationship between iron and silica with their corresponding marginal distributions obtained from the original data set (a) and 3000 randomly selected block values from realisation No. 1 simulated by conventional (b) and proposed (c) algorithms.

Production scheduling

This study analyses the performance of hierarchical cosimulation integrated with inverse transform sampling and two-stage stochastic production scheduling. In that regard, production scheduling results produced by the proposed stochastic strategy are compared to the upper and lower bounds. The upper bound is an optimistic and impossible strategy that shows the best NPV for each realisation. It is computed using MIP on each realisation individually. The lower bound is a deterministic strategy obtained from e-type models of iron and silica. It is an inefficient solution because it involves the risk of sending an extracted material to the wrong destinations. For example, if a block is considered as ore in an e-type model but turns out to be waste, both mining and processing costs are applied to this block. Table 2 lists parameters used for long-term production scheduling. This set of parameters is conceptual and not chosen for this particular deposit, and its objective is to provide the same environment for a fair comparison of the three strategies. Finally, three pushbacks are selected based on the deterministic case after grouping pits and ensuring that each group has a similar tonnage.

TABLE 2
Parameters for production scheduling.

Price (\$/ton)	80.0	Penalisation (\$/ton)	1.5	Mining capacity (ton/day)	153 000
Mining cost (\$/ton)	3.0	Iron threshold (%)	30.0	Processing capacity (ton/day)	130 000
Processing cost (\$/ton)	10.5	Silica threshold (%)	5.0	Slope angle	50°
Selling cost (\$/ton)	30.0	Recovery rate	0.8	# pushbacks	3

In the proposed mine planning solution, pit limits are identified based on e-type values. As a result, the deposit is planned to produce 457 Mton of ore and 69 Mton of waste. Alternatively, the upper bound strategy demonstrates an average of 476 Mton of ore and 49 Mton of waste. Thus, the proposed solution produces a lower amount of ore and a higher amount of waste than the upper bound, which individually implements MIP on each realisation. This can also be observed in ore and waste tonnages for each production period from the proposed solution (Figure 4c). Both parameters are consistent throughout the life-of-mine, while 95 per cent confidence intervals show fair deviations. However, ore tonnages do not reach the full processing capacity of 47.45 Mton/a, unlike the upper bound (Figure 4a) during the first eight years of production. Furthermore, NPV results after each production period calculated with a discount rate of 10 per cent show consistent growth, and the final NPV is between \$458M and \$616M based on a 95 per cent confidence interval. On the other hand, the NPV of the lower bound (Figure 4b) is significantly lower, resulting from sending waste material to the processing plant.

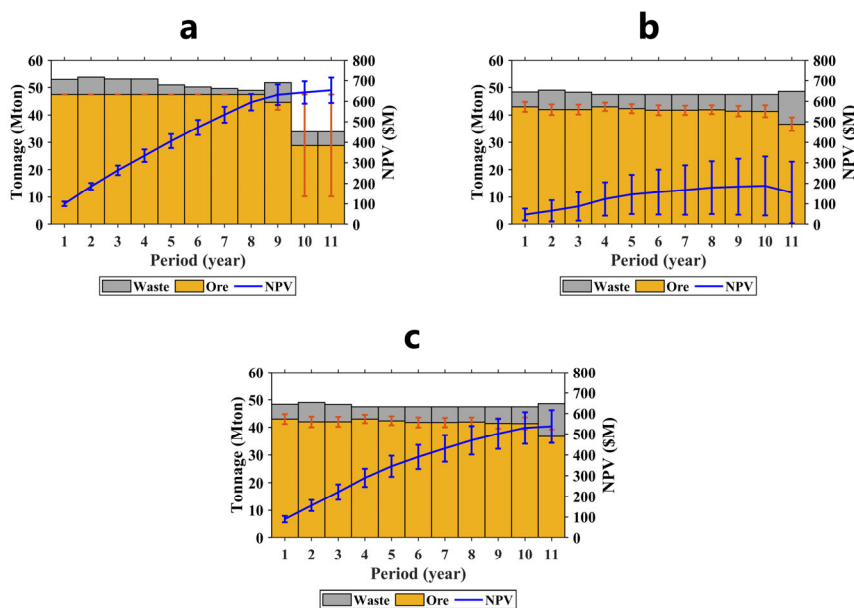


FIG 4 – NPV and tonnage values during each production period with 95 per cent confidence intervals for NPV (blue) and ore tonnage (orange) of the upper bound (a), lower bound (b) and proposed strategy.

NPV results produced by the two-stage stochastic production scheduling are compared to the upper and lower bounds. The average NPV of the upper bound is around \$653M, which is the best NPV for this deposit that is impossible to achieve. On the other hand, the lower bound (ie deterministic case) produces only \$154M because of losses related to sending waste material to the processing plant. And \$537M is reported in the proposed solution. Furthermore, even the worst scenario from the proposed strategy with \$443M NPV is considerably better than the best scenario of the lower bound with \$389M.

Figure 5 shows plots with NPV for 100 realisations for the proposed mine planning solution, upper and lower bounds, which are normalised to the reference plot of the upper bound (ie 100 per cent). By doing so, deviations from the best possible NPV for each realisation can be analysed. The average plot for the proposed solution is at 83 per cent and the lower bound – 24 per cent. Therefore, the NPV of the proposed solution is 17 per cent lower than the upper bound and 59 per cent higher than the lower bound on average.

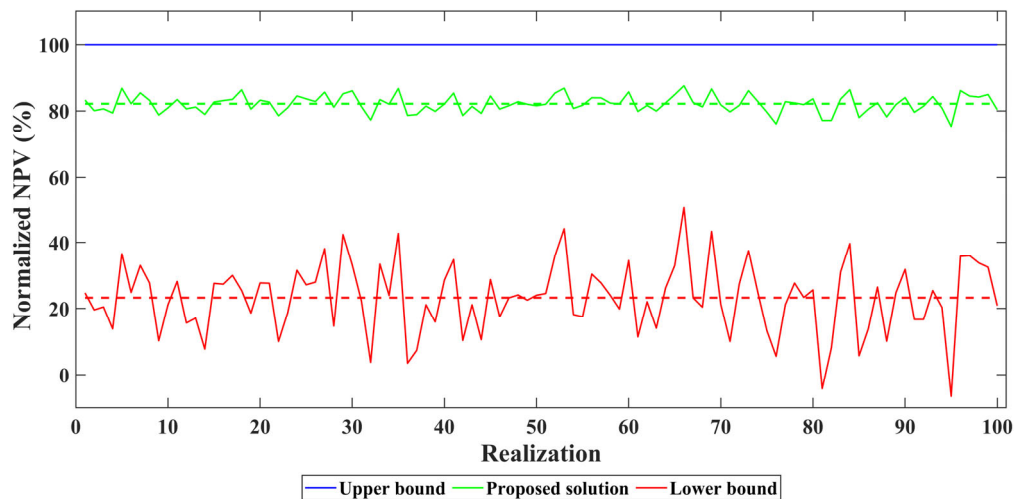


FIG 5 – NPV of the proposed production scheduling strategy compared to the upper and lower bounds for 100 realisations. Plots are normalised to the upper bound (reference case) and dashed lines represent average deviations from the reference plot.

The final analysis is the investigation of the effect of inequality constraint reproduction. Inverse transform sampling prevents the overestimation of silica and increases the economic block values by reducing the cost associated with an impurity content. As a result, optimal pit limits produced using realisations from the proposed cosimulation algorithm contain more profitable blocks. Therefore, NPV increases by 0.76 per cent (Figure 6a) and ore tonnage – by 1.78 per cent (Figure 6b) in comparison to the conventional cosimulation. The absolute benefits from the proposed cosimulation algorithm are 8.39 Mton of ore and \$4.08M NPV.

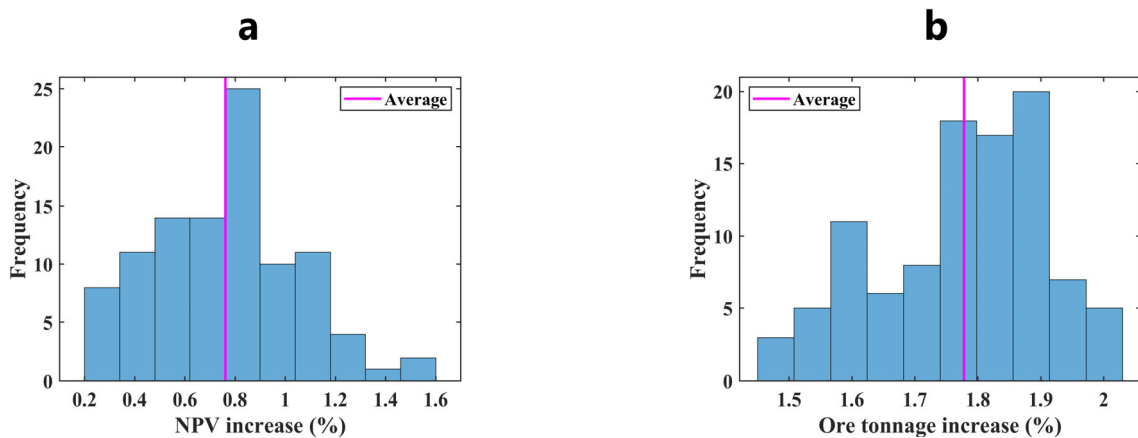


FIG 6 – Histograms of the increase in NPV (a) and ore tonnage (b) in 100 realisations of production scheduling by using the proposed cosimulation algorithm over the conventional one.

CONCLUSIONS

This study shows the economic benefits from inequality constraint reproduction using a case study from an iron deposit composed of iron and silica grades. Poor reproduction of an inequality constraint by the conventional cosimulation methodology leads to an overestimation of silica, which in turn increases losses associated with the impurity content of mined ore. Additionally, although traditional mine planning approaches can maximise NPV, they are unable to manage the risks considering that only a single block model is commonly used as an input. On the other hand, stochastic long-term mine planning approaches generate production schedules with maximised NPV and minimised risks of not meeting production targets.

Iron and silica variables are modelled by the proposed hierarchical cosimulation, which is equipped with an inverse transform sampling to re-simulate faulty values within thresholds from an inequality constraint. Unlike the conventional cosimulation, the proposed methodology perfectly reproduces an

inequality constraint, shows better reproduction of silica histogram and produces a higher correlation coefficient between variables.

Two-stage stochastic production scheduling is proposed to introduce grade uncertainty into mine planning. In this study, first stage decisions obtain fixed production periods using average information from e-type models. Second stage decisions adapt the strategy to multiple unbiased geostatistical scenarios by re-evaluating block destinations. Adaptive block destinations help to minimise the risk of sending an actual waste to a processing plant or valuable ore material to a waste dump. Results are compared with the upper and lower bounds, in which the former is the highest NPV strategy that is also impossible to achieve and the latter is the deterministic strategy. The difference between the upper bound and the proposed solution is 17 per cent, while the lower bound is 59 per cent lower than the proposed solution. Furthermore, the reproduction of an inequality constraint increases NPV by 0.76 per cent or \$4.08M.

It is recommended to apply the proposed methods to other data sets with inequality constraints between two variables. The NPV benefit from reproducing an inequality constraint can be higher when the overestimation of a disturbing element is more substantial. Moreover, the proposed methodology can also be improved by incorporating lithology modelling. For this, the contact analysis can be considered prior to the co-simulation process.

ACKNOWLEDGEMENTS

The first and second authors are grateful to Nazarbayev University for funding this work via Faculty Development Competitive Research Grants for 2018–2020 under Contract No. 090118FD5336. The authors also would like to thank Delphos Mine Planning Laboratory for giving access to MineLink mine planning library.

REFERENCES

- Abildin, Y, Madani, N and Topal, E, 2019. A Hybrid Approach for Joint Simulation of Geometallurgical Variables with Inequality Constraint, *Minerals*, 9(1):24.
- Abulkhair, S and Madani, N, 2021. Assessing Heterotopic Searching Strategy in Hierarchical Cosimulation Framework for Modeling the Variables with Inequality Constraints, *Comptes Rendus Géoscience*, 353(1):115–134.
- Almeida, A S and Journel, A G, 1994. Joint simulation of multiple variables with a Markov-type coregionalization model, *Mathematical Geology*, 26:565–588.
- Arcari Bassani, M A, Costa, J and Deutsch, C V, 2018. Multivariate geostatistical simulation with sum and fraction constraints, *Applied Earth Science*, 127(3):83–93.
- Deutsch, C V, 1989. DECLUS: a fortran 77 program for determining optimum spatial declustering weights, *Computers and Geosciences*, 15(3):325–332.
- Devroye, L, 1986. *Non-Uniform Random Variate Generation* (Springer: New York).
- Dimitrakopoulos, R, 2011. Stochastic optimization for strategic mine planning: A decade of developments, *Journal of Mining Science*, 47:138–150.
- Emery, X, Arroyo, D and Peláez, M, 2014. Simulating Large Gaussian Random Vectors Subject to Inequality Constraints by Gibbs Sampling, *Mathematical Geosciences*, 46:265–283.
- Gershon, M E, 1983. Optimal mine production scheduling: evaluation of large scale mathematical programming approaches, *International Journal of Mining Engineering*, 1:315–329.
- Godoy, M and Dimitrakopoulos, R, 2004. Managing risk and waste mining in long-term production scheduling of open-pit mines, *SME Transactions*, 316:43–50.
- Hochbaum, D S, 2008. The Pseudoflow Algorithm: A New Algorithm for the Maximum-Flow Problem, *Operations Research*, 56(4):992–1009.
- Journel, A G, 1999. Markov Models for Cross-Covariances, *Mathematical Geology*, 31:955–964.
- Leite, A and Dimitrakopoulos, R, 2007. Stochastic optimisation model for open pit mine planning: application and risk analysis at copper deposit, *Mining Technology*, 116(3):109–118.
- Madani, N and Abulkhair, S, 2020. A hierarchical cosimulation algorithm integrated with an acceptance–rejection method for the geostatistical modeling of variables with inequality constraints, *Stochastic Environmental Research and Risk Assessment*, 34(10):1559–1589.

- Moreno, E, Emery, X, Goycoolea, M, Morales, N and Nelis, G, 2017. A two-stage stochastic model for open pit mine planning under geological uncertainty, in *Proceedings of the 38th International Symposium on the Application of Computers and Operations Research in the Mineral Industry* (Colorado School of Mines: Golden).
- Ramazan, S and Dimitrakopoulos, R, 2004. Traditional and New MIP Models for Production Scheduling With In-Situ Grade Variability, *International Journal of Surface Mining*, 18(2):85–98.
- Ramazan, S and Dimitrakopoulos, R, 2013. Production scheduling with uncertain supply: a new solution to the open pit mining problem, *Optimization and Engineering*, 14:361–380.
- Ramazan, S and Dimitrakopoulos, R, 2018. Stochastic optimisation of long-term production scheduling for open pit mines with a new integer programming formulation, in *Advances in Applied Strategic Mine Planning* (ed: R Dimitrakopoulos), pp 139–153 (Springer: Cham).
- Wackernagel, H, 2003. *Multivariate Geostatistics* (Springer: Berlin).